Supplementary Materials: Lower urban humidity moderates outdoor heat stress

T. Chakraborty[1,2,*], Z. S. Venter[3], Y. Qian[2], X. Lee[1,*]

[1]School of the Environment, Yale University, New Haven, CT, USA

[2]Pacific Northwest National Laboratory, Richland, WA, USA

[3]Terrestrial Ecology Section, Norwegian Institute for Nature Research—NINA, 0349 Oslo, Norway

Corresponding Authors: T. Chakraborty (tc.chakraborty@pnnl.gov) and X. Lee (xuhui.lee@yale.edu)

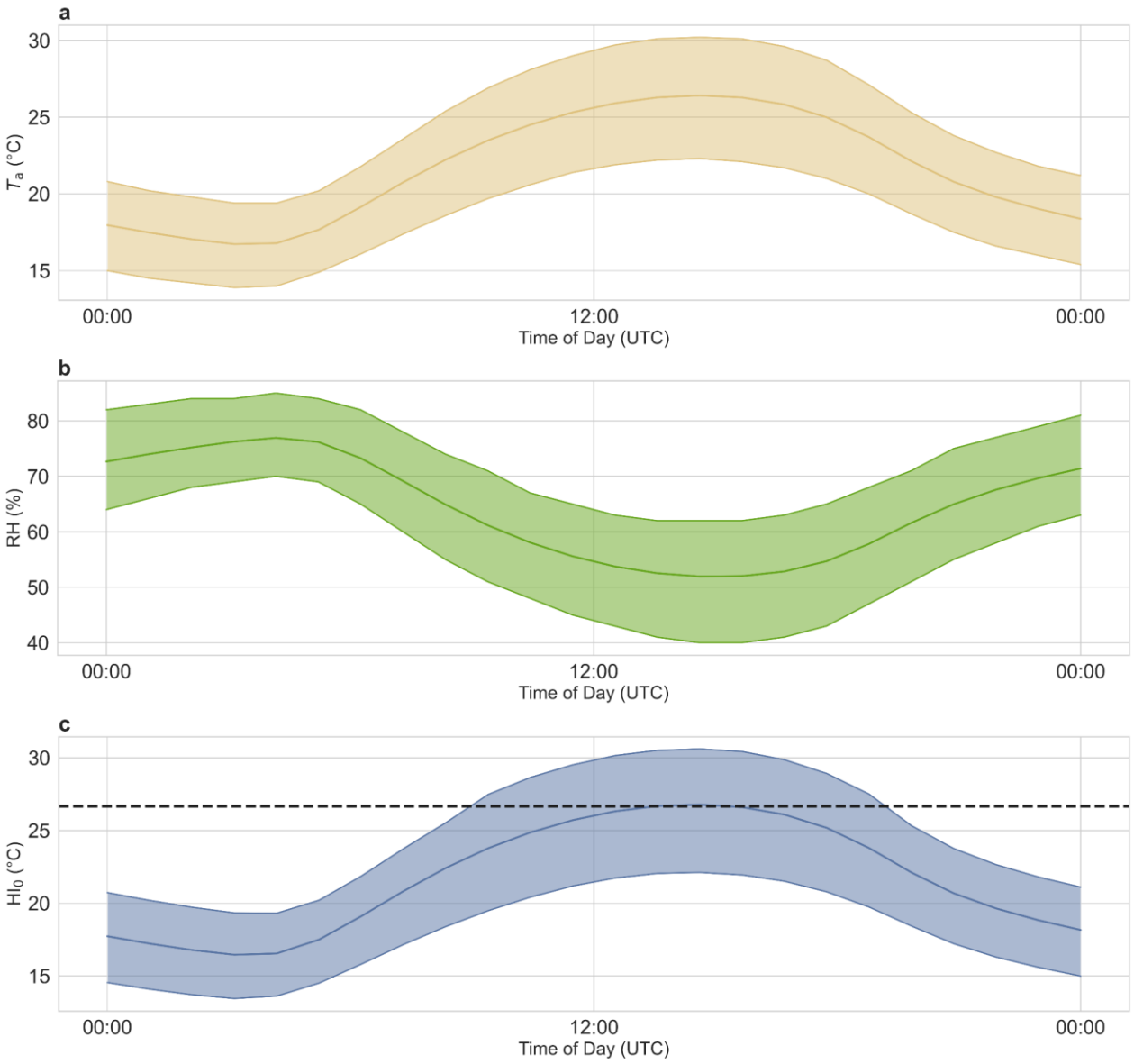

Fig. S1 Diurnal composites of citizen weather station data. Diurnal composites of Netatmo **a** air temperature (T_a), **b** relative humidity (RH), and **c** heat index (HI_0) from all stations in rural buffers considered in the present study. The upper and lower lines represent the 75% and 25% percentile of the measurements, and the middle line is for the mean from all the observations by hour of the day. The dashed horizontal line in sub-figure **c** shows the threshold below which the simplified equation is used for calculating HI_0 (Eq. 1 in Methods).

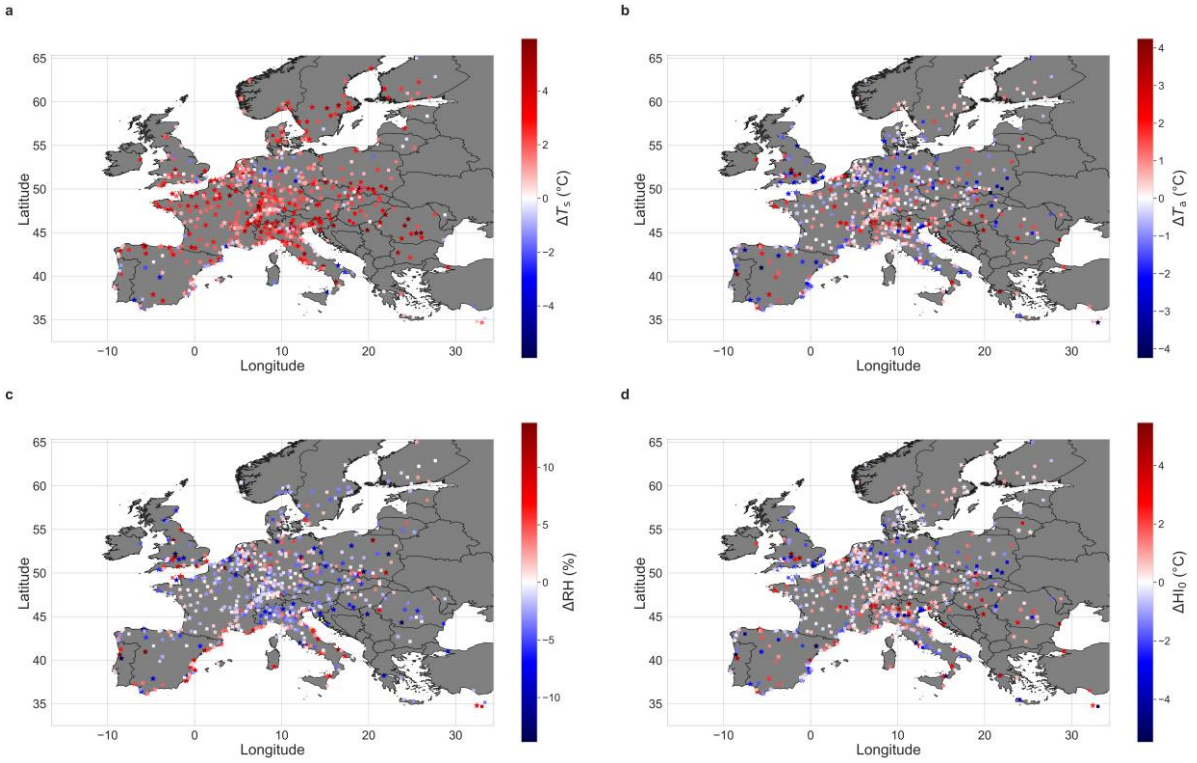

Fig. S2 Urban-rural differences for Terra day across urban clusters in Europe. Spatial distribution of urban-rural differences in **a** surface temperature (ΔT_s), **b** air temperature (ΔT_a), **c** relative humidity (ΔRH), and **d** heat index (ΔHI_0) for urban clusters in Europe with sufficient data corresponding to the Terra satellite daytime overpass (≈10:30 am local time) for July 2019. The stars represent clusters with statistically significant ($p<0.01$) differences between the urban and rural values.

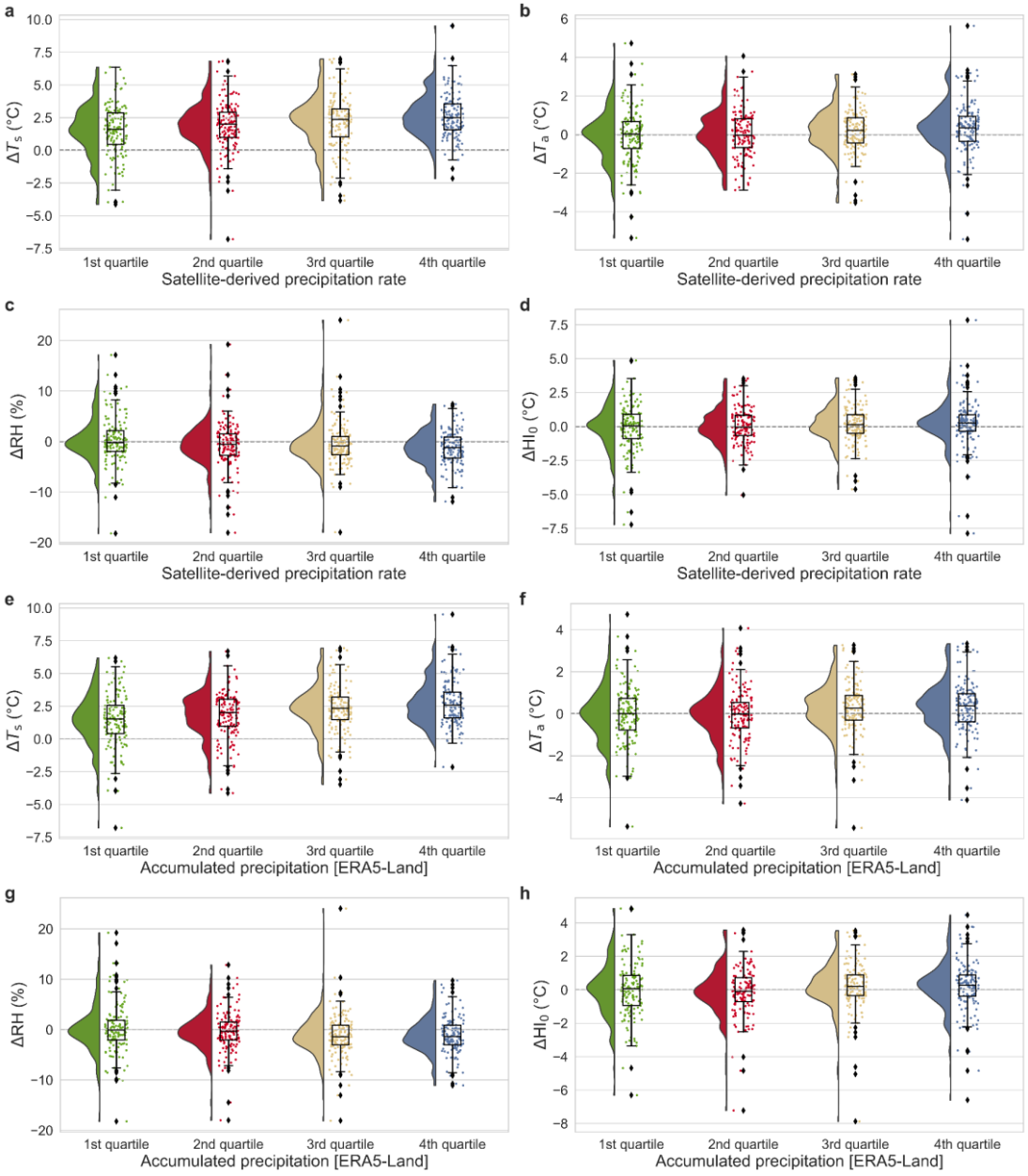

Fig. S3 Urban-rural differences in variables for precipitation quartiles. Distributions of urban-rural differences in **a** surface temperature (ΔT_s), **b** air temperature (ΔT_a), **c** relative humidity (ΔRH), and **d** heat index (ΔHI_0) corresponding to the Aqua daytime overpass (≈1:30 pm local time) for quartiles of satellite-derived precipitation rate in July 2019. Sub-figures **e**, **f**, **g**, and **h** are similar, but use quartiles of accumulation precipitation in July 2019 from the ERA5-Land reanalysis dataset.

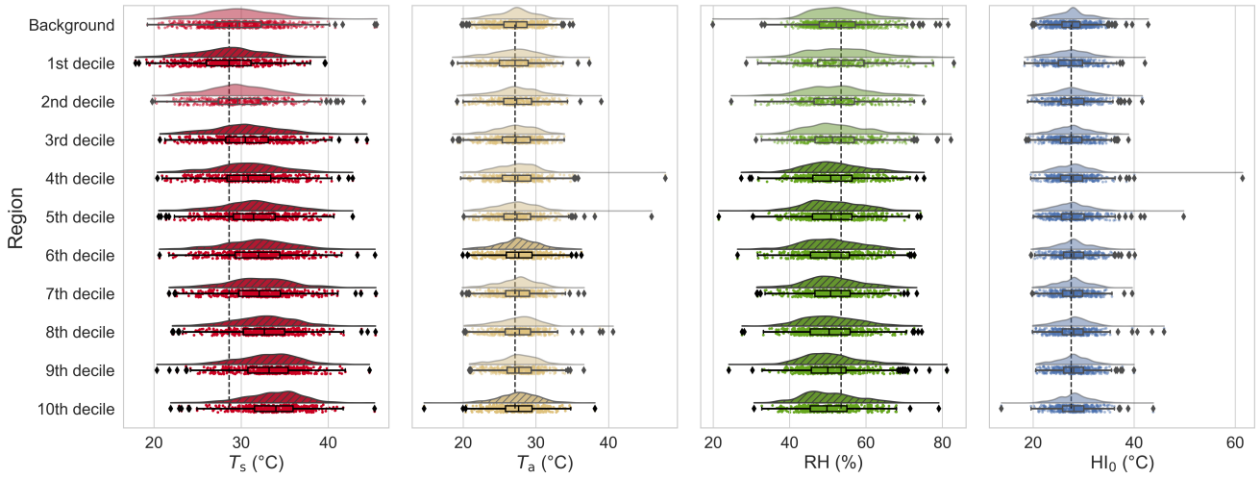

Fig. S4 Intra-urban gradients of variables for Terra day. Distributions of composite mean surface temperature (T_s), air temperature (T_a), relative humidity (RH), and heat index (HI_0) in each of the T_s decile neighborhoods across the urban clusters considered. The vertical dashed lines mark the median of the distribution of the corresponding variable in the 1st T_s decile neighborhood. Decile neighborhoods that show statistically significant ($p<0.01$) differences from the background reference values are shown using hatched density plots and darker shades. All calculations are for the Terra daytime overpass (≈10:30 am local time) for July 2019.

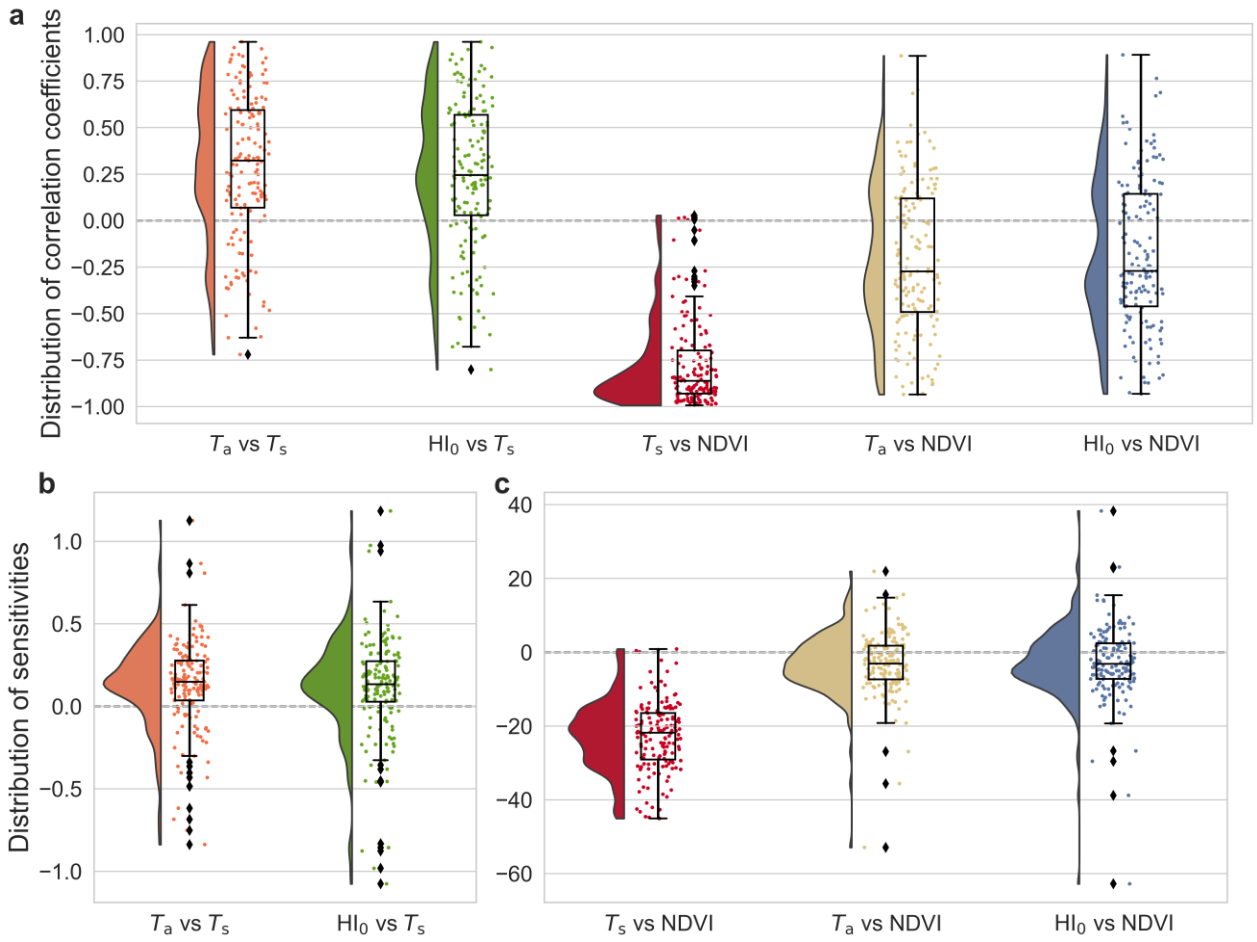

Fig. S5 Associations between variables within urban clusters for Terra day. Sub-fig **a** shows the distributions of the correlation coefficient (r) of linear regressions between surface temperature (T_s) and air temperature (T_a), T_s and heat index (HI_0), Normalized Difference Vegetation Index (NDVI) and T_s, NDVI and T_a, and NDVI and HI_0, respectively, for urban clusters in Europe. Each data point is from a linear regression between pairs of variables for a cluster. The linear regressions have a sample size of ten (one for each T_s decile neighborhood). Sub-fig **b** and **c** show the distributions of the slope of those linear regressions, or the sensitivity of one variable to unit changes in the other. The unit of sensitivity in Sub-fig **c** is °C per unit NDVI. All calculations are for the Terra daytime overpass (≈10:30 am local time) for July 2019.

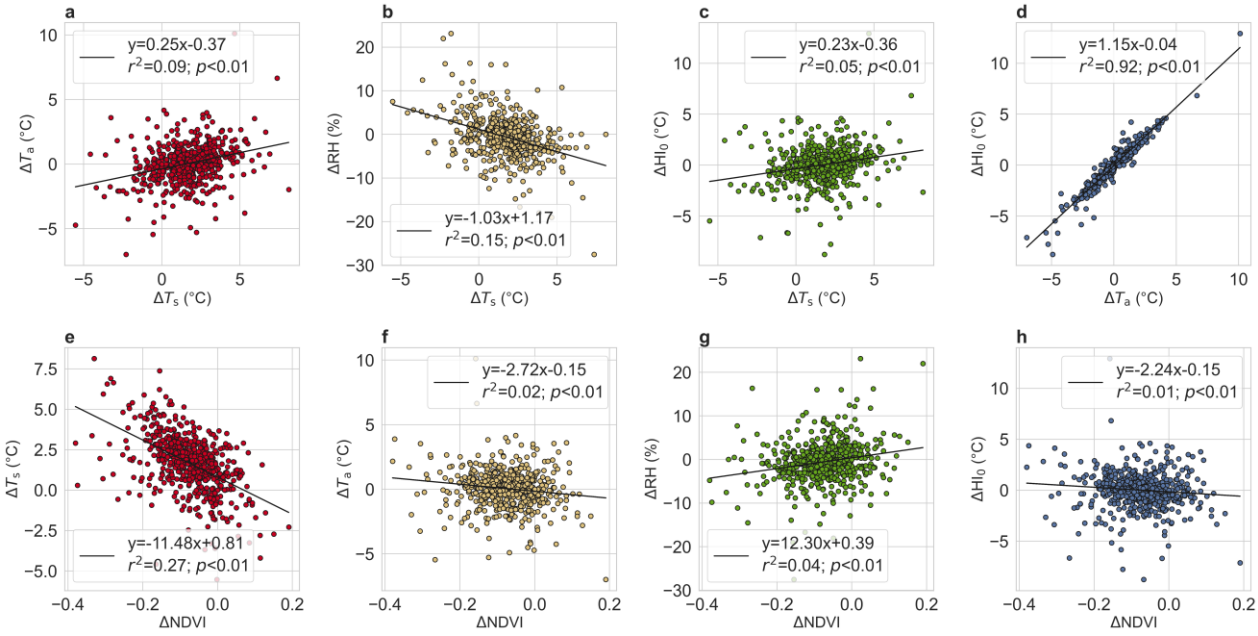

Fig. S6 Associations between variables across urban clusters for Terra day. Associations between urban-rural differences in **a** surface temperature (ΔT_s) and air temperature (ΔT_a), **b** ΔT_s and relative humidity (ΔRH), **c** ΔT_s and heat index (ΔHI_0), **d** ΔT_a and ΔHI_0, **e** Normalized Difference Vegetation Index (ΔNDVI) and ΔT_s, **f** ΔNDVI and ΔT_a, **g** ΔNDVI and ΔRH, and **h** ΔNDVI and ΔHI_0 across urban clusters in Europe. Each dot represents one cluster and the lines and equations of best fit are shown. All calculations are for the Terra daytime overpass (≈10:30 pm local time) for July 2019.

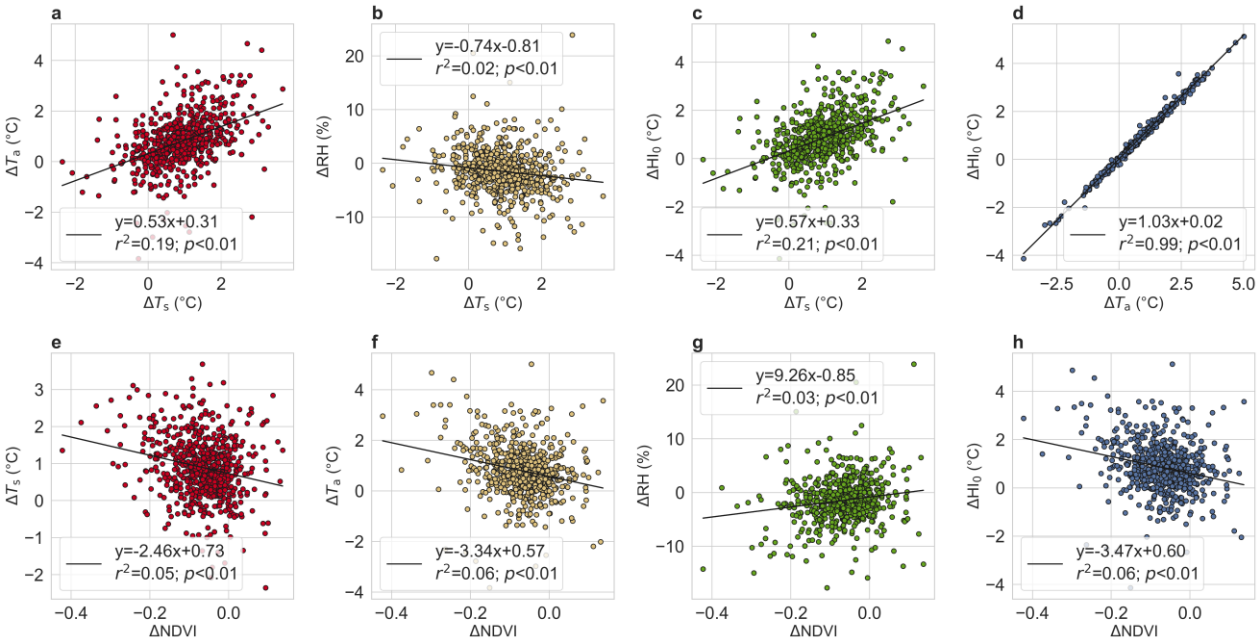

Fig. S7 Associations between variables across urban clusters for Aqua night. Associations between urban-rural differences in **a** surface temperature (ΔT_s) and air temperature (ΔT_a), **b** ΔT_s and relative humidity (ΔRH), **c** ΔT_s and heat index (ΔHI_0), **d** ΔT_a and ΔHI_0, **e** Normalized Difference Vegetation Index (ΔNDVI) and ΔT_s, **f** ΔNDVI and ΔT_a, **g** ΔNDVI and ΔRH, and **h** ΔNDVI and ΔHI_0 across urban clusters in Europe. Each dot represents one cluster and the lines and equations of best fit are shown. All calculations are for the Aqua nighttime overpass (≈1:30 am local time) for July 2019.

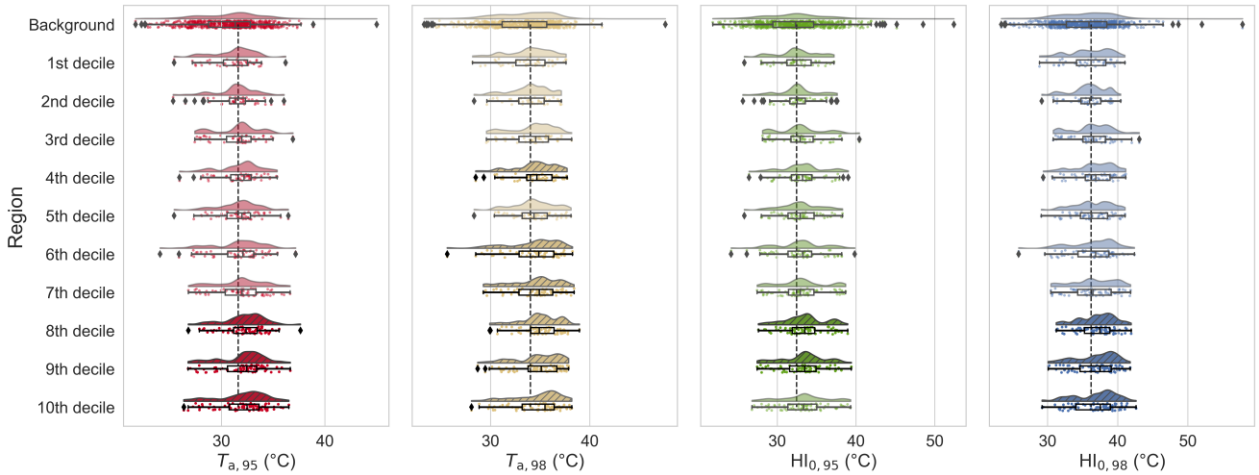

Fig. S8 Intra-urban gradients of extremes. Distributions of the 95th and 98th percentile of hourly observations in July 2019 of air temperature (T_a) and heat index (HI_0) in each of the T_s decile neighborhoods across the urban clusters considered. The vertical dashed lines mark the median of the distribution of the corresponding variable in the 1st T_s decile neighborhood. Decile neighborhoods that show statistically significant ($p<0.01$) differences from the background reference values are shown using hatched density plots and darker shades.

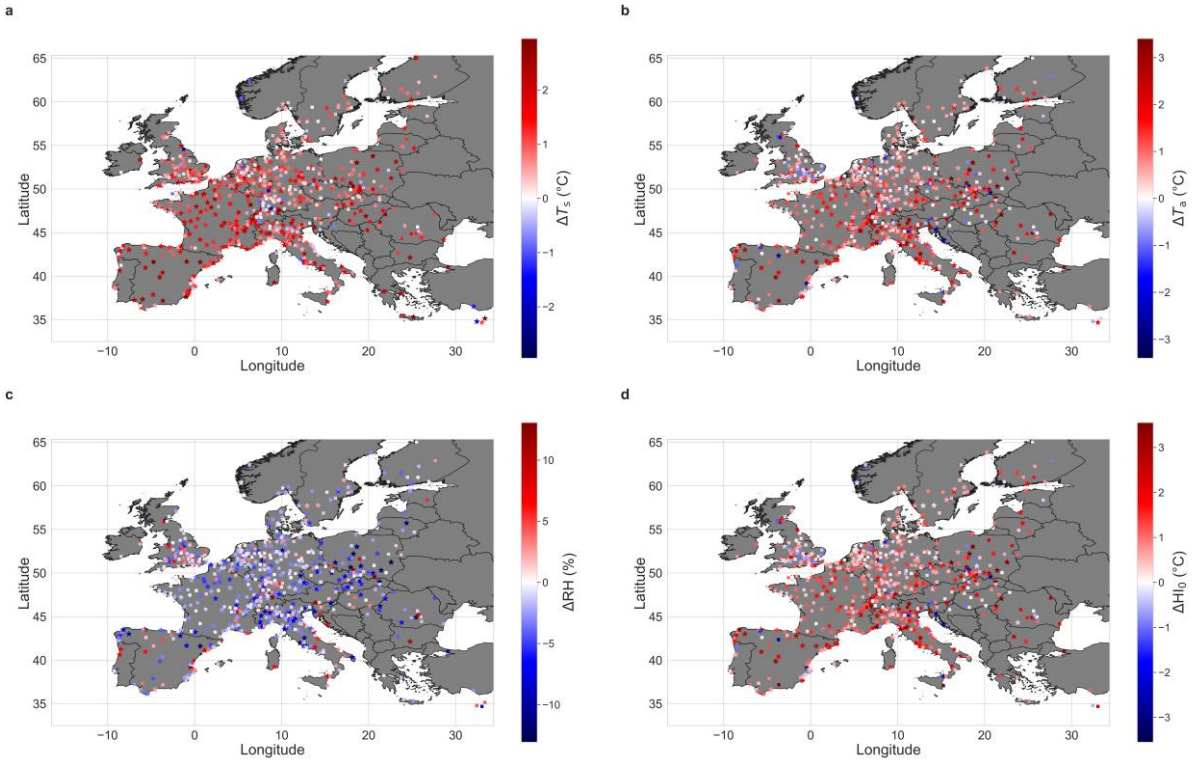

Fig. S9 Urban-rural differences for Aqua night across urban clusters in Europe. Spatial distribution of urban-rural differences in **a** surface temperature (ΔT_s), **b** air temperature (ΔT_a), **c** relative humidity (ΔRH), and **d** heat index (ΔHI_0) for urban clusters in Europe with sufficient data corresponding to the Aqua satellite nighttime overpass (≈1:30 am local time) for July 2019. The stars represent clusters with statistically significant ($p<0.01$) differences between the urban and rural values.

Table S1. P-values of the Mann –Whitney two-sample statistic between the observations corresponding to the Aqua daytime overpass (≈1:30 pm local time) in the background reference region and the observations in the decile neighborhoods for surface temperature (T_s), air temperature (T_a), relative humidity (RH), US National Weather Service heat index (HI_0), four additional estimates of heat index (HI_1 to HI_4), and the humidex for July 2019.

Group	T_s	T_a	RH	HI_0	HI_1	HI_2	HI_3	HI_4	Humidex
1st decile	<0.01	0.16	0.25	0.26	0.21	0.24	0.21	0.18	0.23
2nd decile	0.25	0.23	0.06	0.25	0.27	0.25	0.32	0.23	0.39
3rd decile	0.01	0.43	0.38	0.39	0.40	0.38	0.42	0.41	0.46
4th decile	<0.0001	0.38	<0.01	0.74	0.72	0.74	0.94	0.43	0.91
5th decile	<0.0001	0.09	<0.01	0.25	0.23	0.24	0.34	0.1	0.43
6th decile	<0.0001	0.01	<0.01	0.05	0.05	0.05	0.09	0.02	0.14
7th decile	<0.0001	0.02	<0.0001	0.13	0.11	0.13	0.24	0.03	0.37
8th decile	<0.0001	<0.01	<0.0001	0.05	0.04	0.05	0.11	<0.01	0.20
9th decile	<0.0001	<0.0001	<0.0001	<0.001	<0.001	<0.001	<0.01	<0.0001	<0.01
10th decile	<0.0001	<0.0001	<0.0001	<0.01	<0.01	<0.01	<0.01	<0.0001	0.03

Table S2. P-values of the Mann –Whitney two-sample statistic between the observations corresponding to the Terra daytime overpass (≈10:30 am local time) in the background reference region and the observations in the decile neighborhoods for surface temperature (T_s), air temperature (T_a), relative humidity (RH), US National Weather Service heat index (HI_0), four estimates of heat index (HI_1 to HI_4), and the humidex for July 2019.

Group	T_s	T_a	RH	HI_0	HI_1	HI_2	HI_3	HI_4	Humidex
1st decile	<0.0001	0.27	0.27	0.25	0.27	0.29	0.26	0.28	0.25
2nd decile	0.49	0.41	0.08	0.55	0.58	0.49	0.70	0.44	0.80
3rd decile	<0.001	0.85	0.06	0.86	0.82	0.89	0.60	0.91	0.49
4th decile	<0.0001	0.28	<0.01	0.50	0.58	0.48	0.81	0.32	0.98
5th decile	<0.0001	0.44	<0.001	0.81	0.86	0.74	0.85	0.52	0.70
6th decile	<0.0001	<0.01	<0.0001	0.04	0.04	0.04	0.09	<0.01	0.16
7th decile	<0.0001	0.05	<0.001	0.15	0.17	0.14	0.33	0.07	0.49
8th decile	<0.0001	0.03	<0.0001	0.13	0.14	0.12	0.31	0.04	0.47
9th decile	<0.0001	0.01	<0.0001	0.06	0.07	0.06	0.18	0.02	0.29
10th decile	<0.0001	<0.01	<0.0001	0.03	0.04	0.02	0.09	<0.01	0.16

Table S3. P-values of the Mann –Whitney two-sample statistic between the 95th and 98th percentile of hourly observations in July 2019 of air temperature (T_a) and US National Weather Service heat index (HI_0) for CWSs in the background reference region and the corresponding observations in the decile neighborhoods.

Group	$T_{a,95}$	$T_{a,98}$	$HI_{0,95}$	$HI_{0,98}$
1st decile	0.48	0.36	0.63	0.41
2nd decile	0.40	0.34	0.54	0.69
3rd decile	0.06	0.05	0.15	0.18
4th decile	0.01	<0.01	0.04	0.02
5th decile	0.05	0.03	0.13	0.11
6th decile	0.03	<0.01	0.11	0.06
7th decile	0.01	<0.01	0.06	0.03
8th decile	<0.001	<0.0001	<0.01	<0.01
9th decile	<0.001	<0.0001	<0.01	<0.01
10th decile	<0.001	<0.0001	0.01	<0.01

Table S4. P-values of the Mann –Whitney two-sample statistic between the observations corresponding to the Aqua nighttime overpass (≈1:30 am local time) in the background reference region and the observations in the decile neighborhoods for surface temperature (T_s), air temperature (T_a), relative humidity (RH), US National Weather Service heat index (HI_0), four additional estimates of heat index (HI_1 to HI_4), and the humidex for July 2019.

Group	T_s	T_a	RH	HI_0	HI_1	HI_2	HI_3	HI_4	Humidex
1st decile	<0.0001	0.27	0.12	0.21	0.21	0.20	0.16	0.26	0.14
2nd decile	0.14	0.42	0.01	0.46	0.48	0.30	0.57	0.43	0.61
3rd decile	0.79	0.15	<0.01	0.18	0.18	0.21	0.25	0.16	0.28
4th decile	0.01	0.02	<0.01	0.02	0.02	0.56	0.02	0.02	0.03
5th decile	<0.001	0.01	<0.01	0.01	0.01	0.38	0.02	0.01	0.02
6th decile	<0.0001	<0.0001	<0.0001	<0.0001	<0.0001	0.45	<0.0001	<0.0001	<0.0001
7th decile	<0.0001	<0.0001	<0.0001	<0.0001	<0.0001	0.63	<0.0001	<0.0001	<0.0001
8th decile	<0.0001	<0.0001	<0.0001	<0.0001	<0.0001	0.56	<0.0001	<0.0001	<0.0001
9th decile	<0.0001	<0.0001	<0.0001	<0.0001	<0.0001	0.47	<0.0001	<0.0001	<0.0001
10th decile	<0.0001	<0.0001	<0.0001	<0.0001	<0.0001	0.02	<0.0001	<0.0001	<0.0001